Saudi Journal of Biological Sciences 29 (2022) 2552–2563

Contents lists available at ScienceDirect

Saudi Journal of Biological Sciences

journal homepage: www.sciencedirect.com

Original article

In vitro embryotoxicity and mode of antibacterial mechanistic study of gold and copper nanoparticles synthesized from *Angelica keiskei* (Miq.) Koidz. leaves extract

Chandran Krishnaraj [a,c], Glenn M Young [b], Soon-Il Yun [a,c,*]

[a] Department of Food Science and Technology, College of Agriculture and Life Sciences, Jeonbuk National University, Jeonju 54896, Republic of Korea
[b] Department of Food Science and Technology, University of California, Davis, CA 95616, USA
[c] Department of Agricultural Convergence Technology, College of Agriculture and Life Science, Jeonbuk National University, Jeonju 54896, Republic of Korea

ARTICLE INFO

Article history:
Received 3 July 2021
Revised 13 December 2021
Accepted 14 December 2021
Available online 17 December 2021

Keywords:
Angelica keiskei
Gold nanoparticles
Copper nanoparticles
In vitro embryotoxicity
Zebrafish

ABSTRACT

The present study demonstrated the *in vitro* embryotoxicity assessment of gold nanoparticles (AuNPs) and copper nanoparticles (CuNPs) prepared from the leaves extract of *Angelica keiskei* (Miq.) Koidz. and addressed their mode of antibacterial mechanisms. Both AuNPs and CuNPs were rapidly synthesized and the formations were observed within 1 h and 24 h, respectively. Further the morphological images of the nanoparticles were confirmed through transmission electron microscopy (TEM), field emission scanning electron microscopy (FE-SEM) and atomic force microscopy (AFM). The high-resolution X-ray diffraction (HR-XRD) analysis of the biosynthesized AuNPs and CuNPs were matched with joint committee on powder diffraction standards (JCPDS) file no of 04-0784 and 89-5899, respectively. A strong prominent Au and Cu signals were observed through energy dispersive spectroscopy (EDS) analysis. Fourier transform infrared spectroscopy (FT-IR) analysis confirmed the responsible phytochemicals for the synthesis of AuNPs and CuNPs. In order to assess the toxic effects of AuNPs and CuNPs, bactericidal activity was performed against few of the test pathogens in which the effective inhibition was observed against Gram-negative bacteria than the Gram-positive bacteria. The mode of action and interaction of nanoparticles were performed on the bacterial pathogens and the results concluded that the interaction of nanoparticles initially initiated on the surface of the cell wall adherence followed by ruptured the cells and caused the cell death. In addition to the antibacterial activity, *in vitro* embryotoxicity studies were performed against zebrafish embryos and the results confirmed that 200 μg/ml concentration of AuNPs showed the embryotoxicity, whereas 2 μg/ml of CuNPs resulted the embryotoxicity. Furthermore, the morphological anomalies of zebrafish embryos revealed the toxic nature of the synthesized nanoparticles.

1. Introduction

Angelica keiskei (Miq.) Koidz. (Umbelliferae) plant has been traditionally used as a diuretic, mild cathartic, tonic and galactagogue (Kimura and Baba, 2003). It is also been used as medicine to treat dyschezia, dysgalactia and act to restore vitality (Kil et al., 2017). Commonly, this herb is called as 'Tomorrow's Leaf (Baba et al., 1998) and distributed widely in Asian countries (Park, 2013). The plant parts of *Angelica keiskei* (Miq.) Koidz. were widely used for the food time which serves as a juice and also used for the deep frying (Imai and Imai, 2008), flour (Bao, 2014), wine (Su, 2014), making tea (Liu et al., 2014), and cosmetics (Ku et al., 2014). Currently, the synthesis of Au, Cu, Ag, Se, ZnO and other metal nanoparticles synthesized using the plant leaves extract became rapid and simple process and there is a multiple research work focused on the synthesis of metal nanoparticles such as Au (Krishnaraj et al., 2019), Cu (Ghosh et al., 2020), Ag (Krishnaraj et al., 2010), Se (Cittrarasu et al., 2021) and ZnO (Ogunyemi et al., 2019). Among these, biologically synthesized AuNPs and

* Corresponding author at: Department of Food Science and Technology/Department of Agricultural Convergence Technology, College of Agriculture and Life Sciences, Jeonbuk National University, Jeonju 54896, Republic of Korea.
E-mail addresses: krishnarajbio@gmail.com (C. Krishnaraj), siyun@jbnu.ac.kr (S.-I. Yun).

Peer review under responsibility of King Saud University.

Production and hosting by Elsevier

https://doi.org/10.1016/j.sjbs.2021.12.039
1319-562X/

CuNPs are playing a tremendous role because of their wide applications in biological field (Botteon et al., 2021; Bukhari et al., 2021).

In general, the green synthesis of metal nanoparticles using the plant leaves extract is a non-toxic approach with inexpensive process, having the better antibacterial activity compared to any other chemical compound (Yasmin et al., 2014). In order to synthesize high antibacterial activity of nanoparticles without using any toxic chemicals, in this work AuNPs and CuNPs were synthesized using *Angelica keiskei* (Miq.) Koidz. leaves. Furthermore, AuNPs have received highest interest in research (Schaffler et al., 2014) compared to other metal nanoparticles synthesized from the plant leaves extract. Recently, Anbu et al. (2020) produced 15 nm sizes of AuNPs using *Platycodon grandiflorum* leaves extract and evaluated their antibacterial potential. Similarly, AuNPs had been synthesized from many plant sources like *Coleus amboinicus* (Narayanan and Sakthivel, 2010) and *Vitex negundo* (Veena et al., 2019). In our previous report, we have also synthesized 5–50 nm sizes of AuNPs with anisotropic morphology using *Spinacia oleracea* Linn., leaves extract and evaluated their anticancer activity against mouse myoblast cancer cells (C_2C_{12}) (Ramachandran et al., 2017). Biologically synthesized AuNPs having the strong antimicrobial activity, which enables the electrostatic interaction between the nanoparticles and the surface charge of the bacterial cell wall resulting in membrane distortion, leads to membrane permeability, electron transport, osmoregulation and cell death (Rashmi et al., 2020; Henriquez et al., 2020).

In addition, Cu is acting as a co-factor for enzyme as well as metalloproteins at a low concentration but the increasing concentrations acting as a prominent antibacterial agent by enabling the stop of some important protein functional groups, generating the free radicals, inactivation of essential enzymes and causing the changes in membrane integrity (Abdullah et al., 2018; Rajeshkumar et al., 2019). Recently, few reports demonstrate that the antibacterial activity of CuNPs was due to the accumulation of Cu on the bacterial membrane, cytoplasm and enzymes and thereby proteins and ions release from the cells (Vincent et al., 2016).

Currently, the wide spread uses of AuNPs and CuNPs into biomedical applications were increased because of their potent antimicrobial as well as antioxidant activities (Milanezi et al., 2019; Usman et al., 2013). In addition, there are a number of consumer products introduced into the market with the engineered nanoparticles (Gulson et al., 2010), without knowing the potential risk to the biological systems including human. So, there is a possible chance of leaching the nanoparticles from the end user products due to their smallness in size during or after the usage into the environment, resulting into a serious threat to biotic organisms in the ecosystems (Navarro et al., 2018; Krishnaraj et al., 2012). Hence, there is an urgent need to take the proper mitigation of control measures to assess the toxicity of nanoparticles as well as avoiding their leaching properties into the ecosystem is advisable. There are number of publications worldwide have assessed AuNPs toxicity using the zebrafish embryos (Ramachandran et al., 2017). Very interestingly, few studies reported that biologically synthesized nanoparticles had less toxicity than the chemical synthesis of nanoparticles using embryonic zebrafish (Aerle et al., 2013; Xia et al., 2016). Also, few researches focused on the assessment of toxicity using plant leaves extract based synthesis of silver nanoparticles on adult zebrafish (Krishnaraj et al., 2016). But, to the best of our knowledge, none of the reports exist on the *Angelica keiskei* (Miq.) Koidz. leaves extract based synthesis of AuNPs and CuNPs and their comparative antibacterial mechanisms as well as assessment of *in vitro* embryotoxicity from zebrafish.

2. Materials and methods

The leaves of *Angelica keiskei* were picked from inside the campus of Jeonbuk National University, Jeonju, South Korea. The chemicals like Gold (III) chloride trihydrate ($HAuCl_4{\cdot}3H_2O$), Copper (II) sulfate pentahydrate ($CuSO_4{\cdot}_5H_2O$), Methyl thiazolyl diphenyltetrazolium bromide (MTT) were procured from Sigma Aldrich. Gram-positive bacterial culture of *Bacillus cereus* (ATCC 14579) *Staphylococcus aureus* (KCTC 1927) and Gram-negative bacterial culture of *Escherichia coli* (KCCM 11234) and *Salmonella typhimurium* (ATCC 14028) were procured from American Type Culture Collection and Korean Culture Centre of Microorganisms (KCCM).

2.1. Synthesis of nanoparticles

The known quantity (10 g) of *Angelica keiskei* healthy leaves thoroughly washed with running tap water followed by cleaned with Distilled water ($D{\cdot}H_2O$) several times to remove any unwanted dirt and other materials from the leaves. The cleaned leaves were further boiled in $D{\cdot}H_2O$ (100 ml) in an oven of about 5 min and filtered using Whatman filter paper. Further the 12 ml of the extract added with 38 ml of $D{\cdot}H_2O$ along with 1 mM $HAuCl_4{\cdot}3H_2O$ solution was added slowly and kept in dark for AuNPs formation. Similarly, 12 ml of extract mixed with 38 ml of $D{\cdot}H_2O$ and 10 mM $CuSO_4{\cdot}5H_2O$ was added slowly into the reaction mixture for CuNPs formation. Further the reaction mixture for CuNPs was kept in a shaker at 120 rotated per minute (rpm) speed and the periodic aliquots of the samples were collected for UV–Vis. spectroscopic study. Leaves extract alone maintained throughout the experiment as control setup.

2.2. Optimization of reaction mixtures for nanoparticles formation

The AuNPs and the CuNPs were synthesized from leaves extract of *Angelica keiskei* and the multiple parameters like pH (6–10), concentration of substrate for AuNPs (1–3 mM) and CuNPs (10–30 mM), concentration of leaves extract (6 ml + 44 ml extract; 12 ml + 38 ml extract; 18 ml + 32 ml extract) were optimized in the reaction solution through UV–Vis spectrophotometer for a rapid and controlled synthesis of nanoparticle.

2.3. Nanoparticles characterization

Synthesized nanoparticles were purified through high speed ultracentrifugation at 15,000 rpm for 20 min and the supernatants were discarded. Then the pellets were dissolved in 1 ml of deionized water and the resulting aliquots containing nanoparticles were used for various characterization techniques like TEM, AFM, FE-SEM and EDS analyses. Twenty-five μl of the aliquots containing AuNPs and CuNPs were fixed on a grid of TEM and captured the images through TEM (Hitachi H-7650) and the dried samples were surface coated on carbon tape and observed through FE-SEM (Carl Zeiss SUPRA40VP). The presence of metals in the aliquots were observed through EDS analysis (Carl Zeiss SUPRA40VP). In addition, the size, surface topography and 3D images of the synthesized nanoparticles were confirmed through AFM (Bruker Multimode 8). Further, the AuNPs and CuNPs reaction aliquots were freeze dried (Model No: MCF D8512). The obtained powders of AuNPs and CuNPs were dissolved in $D{\cdot}H_2O$ (1 mg/ml conc.) and used for antibacterial mechanisms as well as embryotoxicity assessment studies. Then the dried powders were further subjected to glass slide coating for HR-XRD (Bruker D8 Advance) and KBr pelletizer method for FT-IR analysis (Perkin Elmer model).

2.4. Antibacterial activity against Gram-positive and Gram-negative bacteria

The AuNPs and CuNPs were tested for their antibacterial activity against the pathogens.

2.4.1. Well diffusion assay

The test bacterial strains of Gram-positive *Bacillus cereus, Staphylococcus aureus* and the Gram-negative *Escherichia coli, Salmonella typhimurium* were grown in nutrient broth. Then the nutrient agar plates were prepared and the spread plate techniques were followed. Using the sterile cork borer 6 wells were made into agar plates and each well were filled with sterile $D{\cdot}H_2O$ (control) and 40 μg/ 40 μl conc. of plant extract, $HAuCl_4{\cdot}3H_2O$, AuNPs, $CuSO_4{\cdot}5H_2O$ and CuNPs and incubated the plates at 37 ± 2 °C for 12–24 h.

2.4.2. Bactericidal kinetic study

One ml of the test bacterial cultures was aseptically transferred into 100 ml of the sterile (Muller Hinton Broth) MHB in 250 ml flasks and 1 ml of 1 mM conc. of $AuCl_4{\cdot}3H_2O$ followed by 1 mg/ml conc. of AuNPs, CuNPs, plant extract and 1 ml of 10 mM conc. of $CuSO_4{\cdot}5H_2O$, positive control (media alone without bacteria) and negative control (bacteria alone without treatment) were inoculated separately into the broths. The setup was kept at 37 °C under shaking condition with a speed of 120 rpm and the readings were noted at every 4 h intervals at 600 nm for up to 24 h.

2.4.3. Minimum inhibitory concentration

The MIC of AuNPs and CuNPs were studied using the standard published protocol of 96 well plate (SPL Life sciences, Korea) with a little modification (Krishnaraj et al., 2010). Briefly, 100 μl of the nutrient broth medium added into suitable well in a 96 well plate followed by 40 μg/40 μl conc. of $HAuCl_4{\cdot}3H_2O$, AuNPs, $CuSO_4{\cdot}5H_2O$ and CuNPs were added into first well of each column followed by serial dilutions were made up to 12 wells in a row and discarded the final solutions. One hundred μl of the test pathogens were inoculated into each well and incubated at 37 °C for 12 h. Finally, 5 μl of 0.5% MTT solution was added to each well and the readings were noted using ELISA reader at OD_{595}.

2.4.4. Antibacterial mechanisms of nanoparticles

The log phase cultures of the test bacterial pathogens (10 ml) were centrifuged using high speed ultracentrifugation at 6000 rpm for 10 min and the pellets collected. Further the pellets containing bacteria was dissolved in sterile $D{\cdot}H_2O$ and 5 ml of these suspensions were mixed with 1 ml of AuNPs and CuNPs separately for each organism and incubated at 37 °C for 8 h. Finally, the reaction solutions were placed in TEM grid and allowed to air dry and observed under Bio-TEM.

2.5. Assessment of embryotoxicity using zebrafish

The toxic effect of biologically synthesized AuNPs and CuNPs were assessed through Fish Embryo Acute Toxicity (FET) test in accordance with OECD test guideline 236, using zebrafish embryos (Lammer et al., 2009). Briefly, the average weight (0.3 ± 0.02 g) and length (24 ± 0.2 mm) of both sexes of zebrafish were used. The commercially purchased artemia were given as feed twice in a day and maintained the fishes in an aquarium of 14 h:10 h light dark cycle for 21 days at a temperature of 28 ± 1 °C and used for breeding the embryo. The breeding chamber containing 1:1 ratio of male and female was kept separately with a divider and sufficient water maintained under static condition in an aquarium before the light switched off in the evening. Further the divider was removed immediately after the light on in the morning and allowed for breeding. The settled embryos on the bottom of the breeding chamber were further transferred into E3 medium ($D{\cdot}H_2O$ with 5 mM NaCl, 0.17 mM KCl, 0.33 mM CaCl, 0.33 mM $MgSO_4$) (Cassar et al., 2019) and incubated at 28.5 °C for 3 h post fertilization (hpf). Further the freshly laid healthy zebrafish embryos were transferred into 24-well plate along with 2 ml of E3 medium. Five concentration of $HAuCl_4{\cdot}3H_2O$ (1 to 20 μg/ml), AuNPs (50 to 250 μg/ml), $CuSO_4{\cdot}5H_2O$ and CuNPs (1 to 5 μg/ml) were loaded to the wells and incubated at 28.5 °C for 72 h. Control embryos were maintained without having any treatment and the tests were performed thrice. The hatching rate as well as mortality and malformations were noted using stereomicroscope. Further the rate of mortality was noted and displayed as the number of dead embryos after 72 hpf. In addition, the morphological anomalies like yolk sac edema, delayed development, mal formation in tail, chorion with debris and lack of movement was observed at 24 hpf.

2.6. Statistical analysis

All the experiments were conducted in triplicate and the data were presented in terms of average value ± standard deviation.

3. Results

3.1. Nanoparticles formation

Twelve ml of the extract along with 38 ml of $D{\cdot}H_2O$ and 1 mM $HAuCl_4{\cdot}3H_2O$ at pH 8 was found to be suitable for rapid synthesis of AuNPs. The characteristic absorption peak of 540 nm was observed within 1 h through UV–Vis spectrum (Fig. 1) and the formation was physically confirmed by change in color of the aqueous extract medium into pinkish violet color (Supplementary Fig. S1a). Similarly, 12 ml of the extract along with 38 ml of $D{\cdot}H_2O$ and 10 mM $CuSO_4{\cdot}5H_2O$ at pH 7 and 8 was found to be suitable for rapid synthesis of CuNPs. The characteristic absorption peak of 327 nm was observed within 24 h through UV–Vis spectrum (Fig. 2) and the formation was physically confirmed by change in color of the aqueous extract medium into green color (Supplementary Fig. S1b). In addition, the control setup (leaves extract) did not show any color change (Supplementary Fig. S1c).

3.2. Instrumentation techniques used for characterizing the nanoparticles

TEM and FE-SEM studies confirmed the presence of polydisperse AuNPs and CuNPs. The size of the synthesized AuNPs were observed around 20 to 40 nm with a spherical and triangular in shapes (Fig. 3a & b) and the spherical shape with an average size of 20 to 60 nm were observed for CuNPs (Fig. 3d & e). A strong prominent signal for Au (Fig. 3c) and Cu (Fig. 3f) in the reaction solution was achieved through EDS spectrum. The morphological topography and the 3D images of the synthesized AuNPs (Fig. 4a, b) and CuNPs (Fig. 4c, d) were studied through AFM and the results confirmed the presence of polydisperse nanoparticles with an average size of 40 nm for AuNPs and 56 nm for CuNPs. The crystalline phase of the synthesized AuNPs and CuNPs were achieved through HR-XRD analyses. Fig. 5a shows the HR-XRD analysis of polycrystalline nature of the synthesized AuNPs which illustrates the fcc of the planes indexed to (111), (200), (220) and (311) matched with JCPDS file No.04-0784. Fig. 5b shows the HR-XRD pattern of synthesized CuNPs illustrates the characteristic diffraction planes indexed to (110), (111), (220), (800) and (713) of fcc matched with JCPDS file No. 89-5899. The bio reduced AuNPs and CuNPs using the aqueous leaves extract of *Angelica keiskei* were further subjected to FTIR analysis to confirm the functional

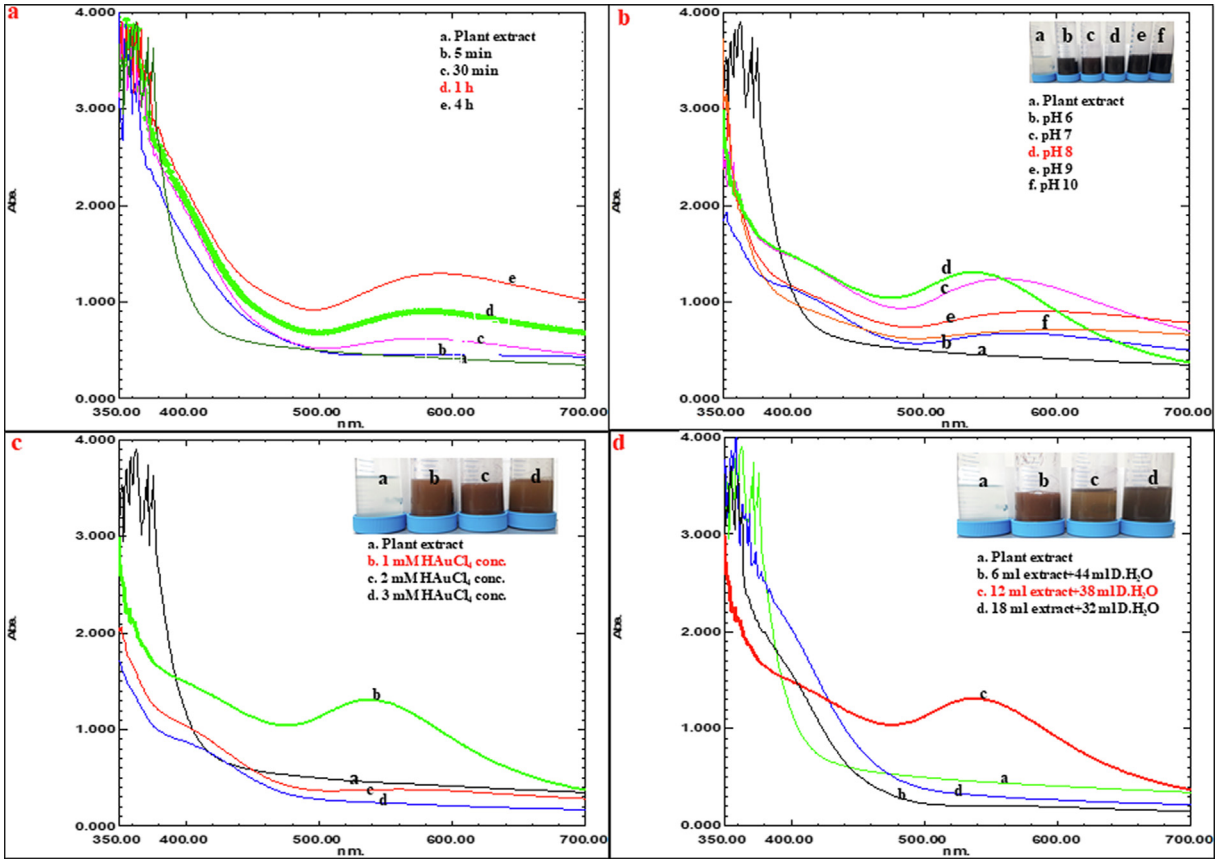

Fig. 1. Optimization process for the biological synthesis of AuNPs (a) different time intervals (b) different pH (c) different substrate conc. (d) different leaves extract conc.

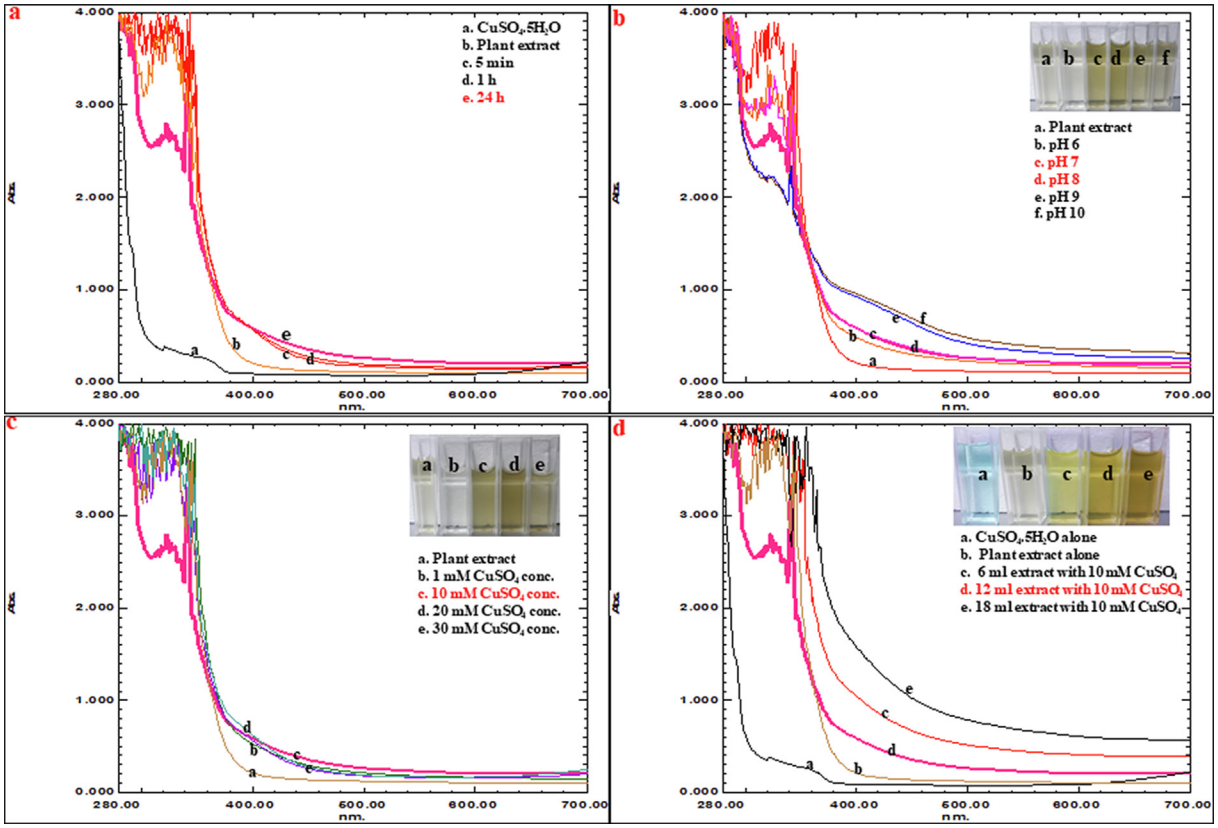

Fig. 2. Optimization process for the biological synthesis of CuNPs (a) different time intervals (b) different pH (c) different substrate conc. (d) different leaves extract conc.

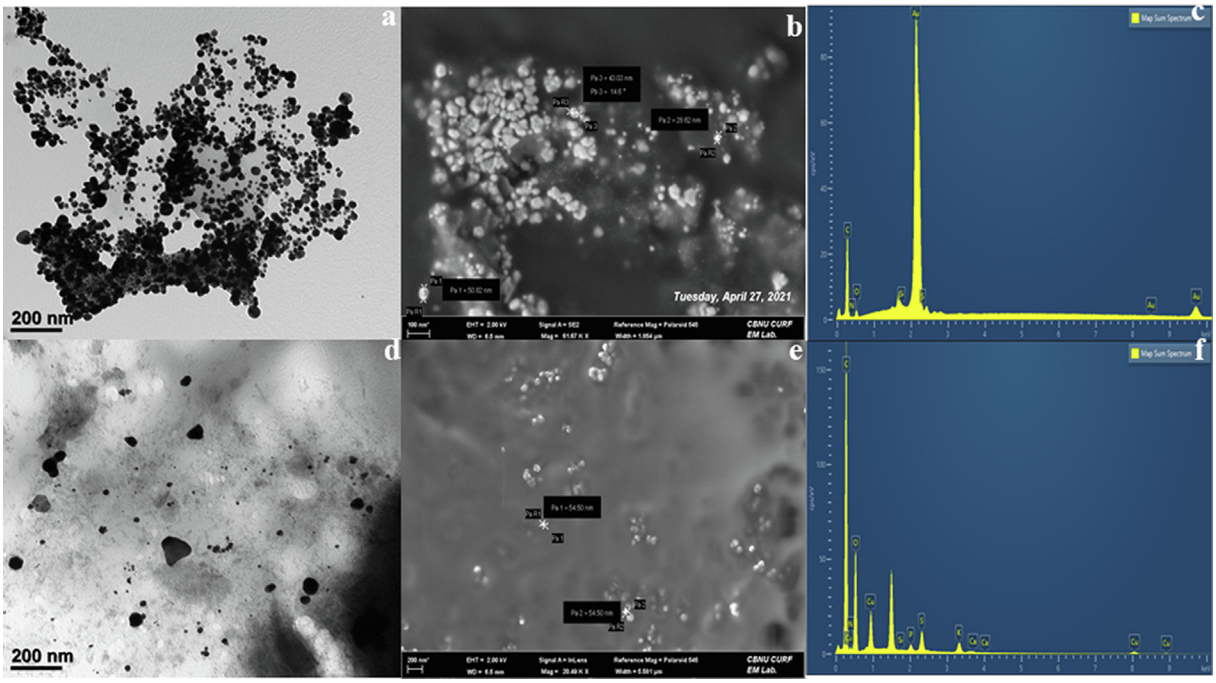

Fig. 3. Electron microscopic images of (a) AuNPs from transmission electron microscope (b) AuNPs from field emission transmission electron microscope (c) energy dispersive spectroscopic analysis of AuNPs (d) CuNPs from transmission electron microscope (e) CuNPs from field emission transmission electron microscope (f) energy dispersive spectroscopic analysis of CuNPs.

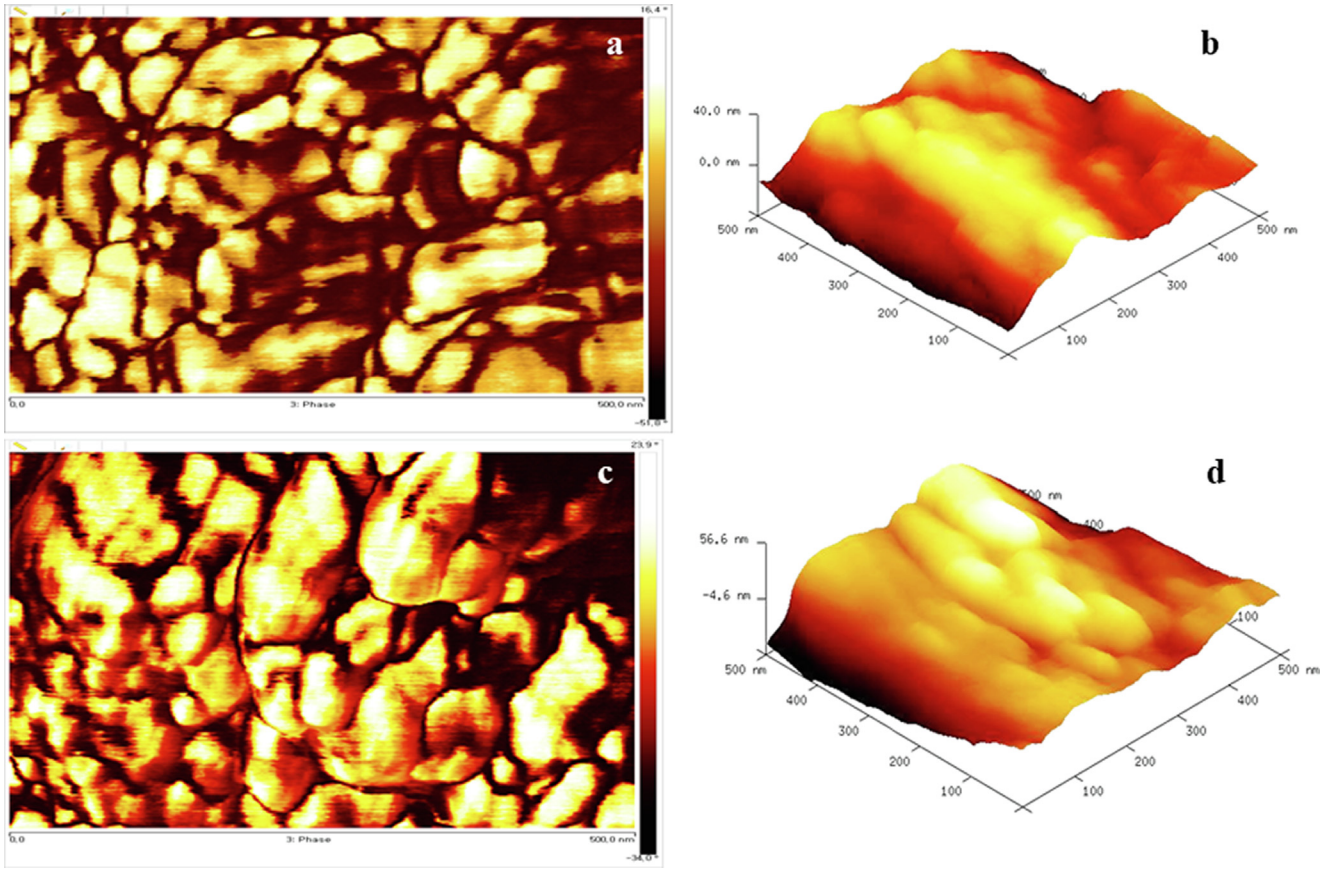

Fig. 4. Atomic force microscopic images of (a) morphological topography of AuNPs (b) 3D image of AuNPs (c) morphological topography of CuNPs (d) 3D image of CuNPs.

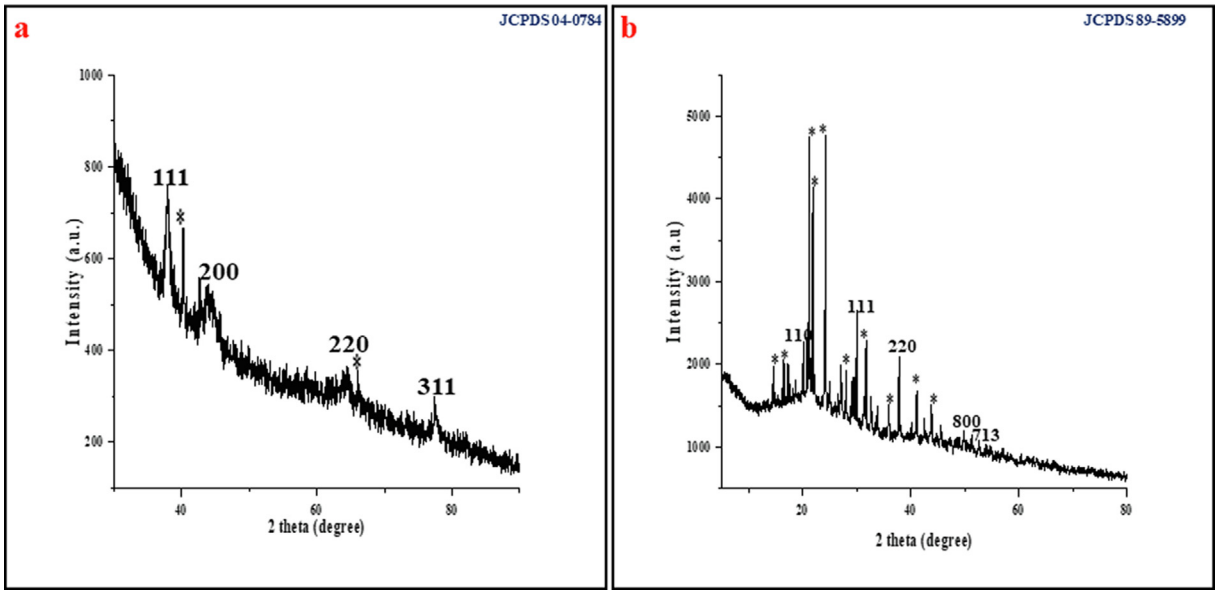

Fig. 5. High resolution X-ray diffraction spectra of (a) AuNPs (b) CuNPs. *peaks indicate the presence of biomolecules.

and active groups. Fig. 6a depicts the FTIR spectra of the leaves extract alone. The high content of active substances with the strong anti-oxidant activity of leaves extract was supported for the reduction of $HAuCl_4{\cdot}3H_2O$ to AuNPs (Fig. 6b). Further, the FTIR spectra of CuNPs confirmed that –NH and –COO groups in the leaves extract of *Angelica keiskei* played a major role in binding of active substances with the copper and thereby equilibrate the nanoparticles biosynthesis (Fig. 6c). The possible mechanism behind the biogenic synthesis of AuNPs and CuNPs was given in the Supplementary Fig. S4.

3.3. Mode of action of antibacterial mechanisms

3.3.1. Antibacterial study

The maximum zone of inhibition was observed in CuNPs and $HAuCl_4{\cdot}3H_2O$ against Gram-negative bacterium, *Escherichia coli* followed by $CuSO_4{\cdot}5H_2O$ and AuNPs. For *Salmonella typhimurium*, the maximum zone of inhibition was observed for CuNPs and $CuSO_4{\cdot}5H_2O$ followed by AuNPs and $HAuCl_4{\cdot}3H_2O$ solution. Similarly, for Gram-positive bacteria such as *Staphylococcus aureus*, the maximum zone of inhibition was observed for CuNPs and $CuSO_4{\cdot}5H_2O$ followed by AuNPs and $HAuCl_4{\cdot}3H_2O$ solution. The CuNPs and $HAuCl_4{\cdot}3H_2O$ solution pronounced a strong antibacterial activity than AuNPs and $CuSO_4{\cdot}5H_2O$ against *Bacillus cereus*. Interestingly, there was no zone of inhibition observed against the plant extract and control well (Supplementary Fig. S5 and Table 1).

3.3.2. Growth curve study

Growth curve study was performed to determine the bacterial survival rate against the treatment of $HAuCl_4{\cdot}3H_2O$, AuNPs, $CuSO_4{\cdot}5H_2O$, CuNPs and plant extract. Based on the results obtained during the treatment of O.D at 600 nm, CuNPs, $CuSO_4{\cdot}5H_2O$ and $HAuCl_4{\cdot}3H_2O$ reaction solutions were retarded more than 50% growth rate at 24 h time interval for *Salmonella typhimurium, Bacillus cereus* and *Staphylococcus aureus*. But in case of AuNPs the growth retardation rate was not much impressive and observed less than 50% growth retardation at 24 h time interval against all the tested pathogens. In addition, $HAuCl_4{\cdot}3H_2O$ solution showed pronounced growth retardation for *Escherichia coli* at 24 h time interval compared to all other tested reaction mixtures (Fig. 7).

3.3.3. Minimum inhibitory concentration

MIC study was performed to understand the effective inhibitory concentration of nanoparticles against the tested pathogens. The effective MIC was observed for $CuSO_4{\cdot}5H_2O$ and CuNPs against *Salmonella typhimurium* (10 μg/10 μl) followed by *Bacillus cereus*, *Staphylococcus aureus* (20 μg/20 μl) and *Escherichia coli* (40 μg/40 μl). But in case of $HAuCl_4{\cdot}3H_2O$, the effective MIC of 20 μg/20 μl was observed against *Salmonella typhimurium, Bacillus cereus* and *Staphylococcus aureus* followed by *Escherichia coli* (40 μg/40 μl). Similarly, the effective MIC of AuNPs against all the tested pathogens was observed at 40 μg/40 μl concentration.

3.3.4. Antibacterial mechanisms through Bio-TEM

In order to understand the antibacterial mechanisms of synthesized AuNPs and CuNPs, Bio-TEM analysis was performed against Gram-positive bacteria of *Bacillus cereus*, *Staphylococcus aureus* and Gram-negative bacteria of *Escherichia coli* and *Salmonella typhimurium*. The bacterial cultures were mixed with 1 ml of as-synthesized AuNPs and CuNPs separately for 8 h. followed by

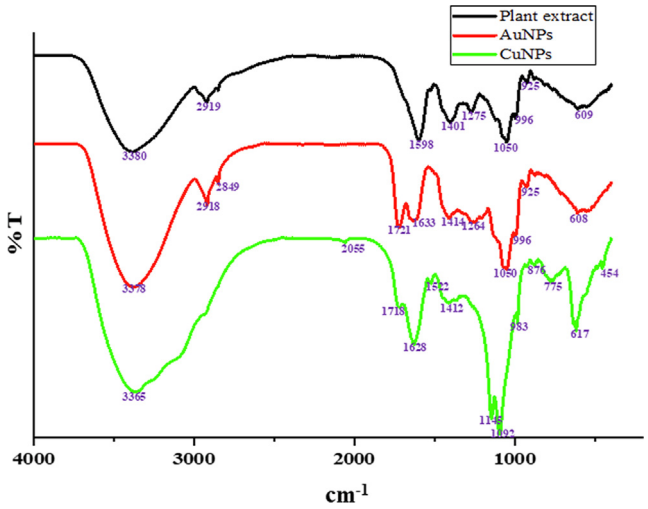

Fig. 6. Fourier transform infrared spectral analysis of (a) plant extract (b) AuNPs (c) CuNPs.

Table 1
Well diffusion assay of biologically synthesized AuNPs and CuNPs from *Angelica keiskei* (Miq.) Koidz leaves extract.

Bacterial pathogens	ZOI (mm in diameter)					
	Control (Sterile D·H_2O)	Plant extract (40 μg/ 40 μl)	$HAuCl_4·3H_2O$ (40 μg/ 40 μl)	AuNPs (40 μg/ 40 μl)	$CuSO_4·5H_2O$ (40 μg/ 40 μl)	CuNPs (40 μg/ 40 μl)
Gram-positive						
Staphylococcus aureus	NZ	NZ	9	10	15	17
Bacillus cereus	NZ	NZ	12	10	10	12
Gram-negative						
Escherichia coli	NZ	NZ	18	10	16	18
Salmonella typhimurium	NZ	NZ	10	10	14	15

NZ no zone formation.

placed in TEM grid, allowed to air dried and observed under Bio-TEM which clearly evident the mechanisms of interaction of nanoparticles initially initiated on the surface of the cell wall adherence followed by rupturing the cells and caused the cell death. Fig. 8a-d shows the Bio-TEM analysis of AuNPs interacted with the test pathogens and Fig. 8e-h shows the Bio-TEM analysis of CuNPs interacted with the test pathogens. The overall proposed antibacterial mechanisms were presented in Supplementary Fig. S6.

3.4. Toxicity studies by zebrafish embryos

3.4.1. Mortality study

Different concentration of biologically synthesized AuNPs, CuNPs along with suitable substrates like $HAuCl_4·3H_2O$, $CuSO_4·5H_2O$ were used to perform the rate of mortality of zebrafish embryos. The obtained results clearly revealed that the increasing concentration leads to increase in mortality rate. The 100% mortality was achieved for $HAuCl_4·3H_2O$ at 15 μg/ml conc. (Fig. 9a). Similarly, for AuNPs it was observed at 200 μg/ml (Fig. 9b). But in case of $CuSO_4·5H_2O$ and CuNPs, 100% mortality was observed at 2 μg/ml concentration (Fig. 9c & d).

3.4.2. Morphological study

The untreated control zebrafish embryo was found to be alive with normal in structure without having any notable observations (Fig. 10a). But in case of $HAuCl_4·3H_2O$, 100% mortality rate was observed at 15 μg/ml conc. whereas in lesser conc. like 5 and 10 μg/ml delayed the hatching compared to control. In addition, the reddish-purple color coagulation of the embryo was observed at the increasing concentrations (Fig. 10b). Interestingly, 100% of the mortality rate was observed for the synthesized AuNPs at

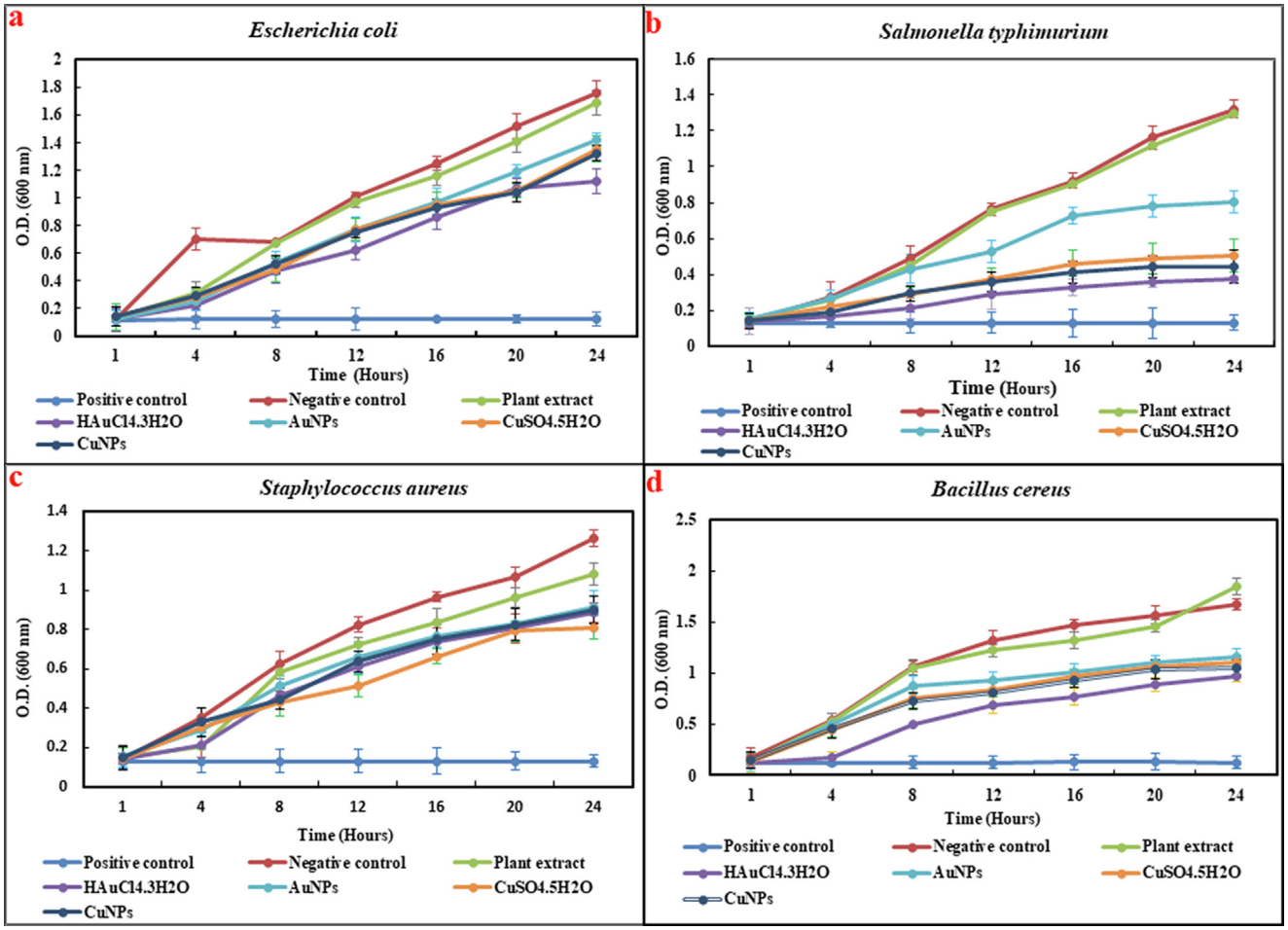

Fig. 7. Growth curve studies of *(a) Escherichia coli (b) Salmonella typhimurium (c) Staphylococcus aureus (d) Bacillus cereus.*

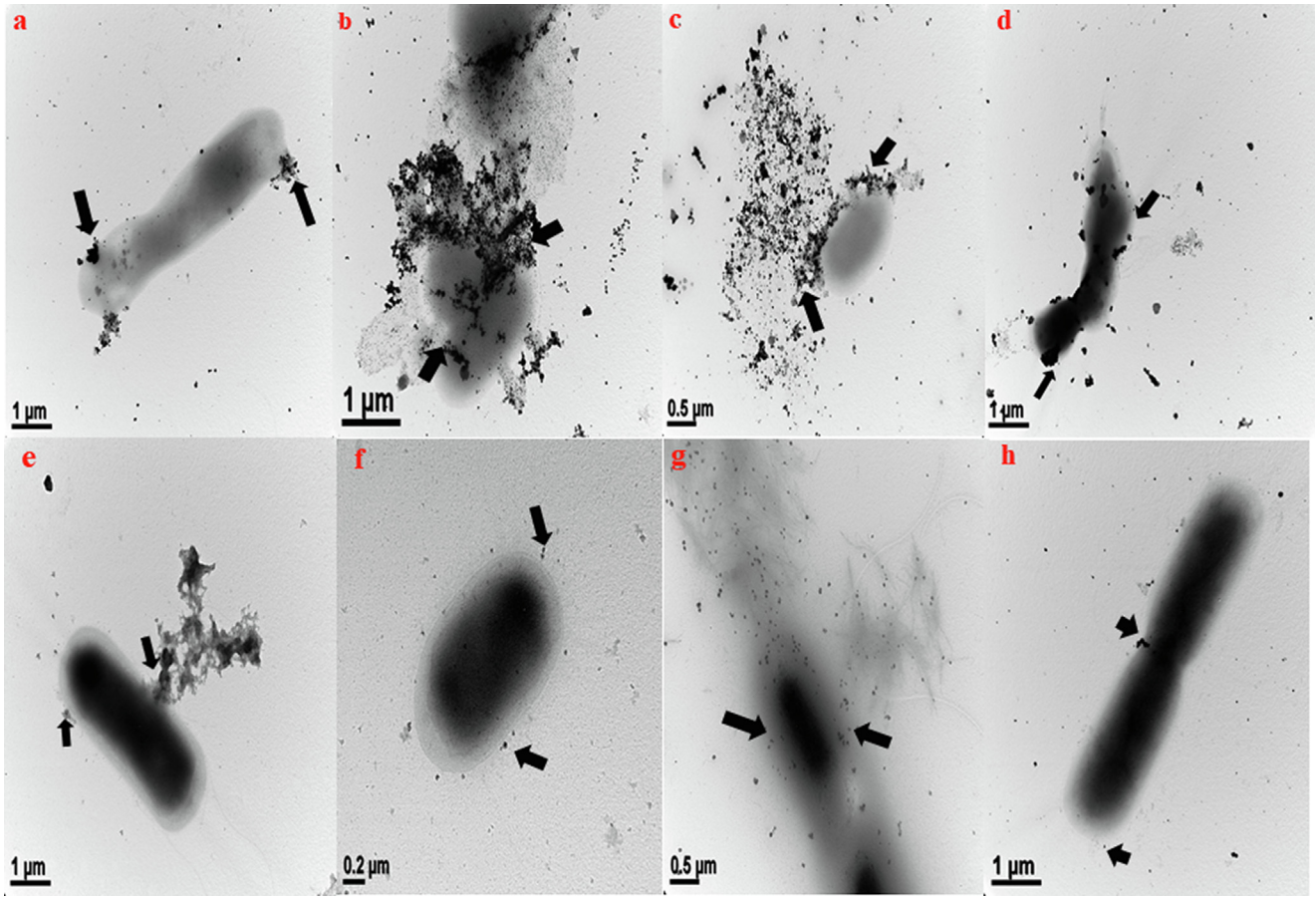

Fig. 8. Mode of interactions of AuNPs (a-d) and CuNPs (e-h) against Gram-positive and Gram-negative bacterial pathogens. *(a) Bacillus cereus (b) Salmonella typhimurium (c) Staphylococcus aureus (d) Escherichia coli (e) Bacillus cereus (f) Salmonella typhimurium (g) Staphylococcus aureus (h) Escherichia coli.* Arrows indicates the presence of nanoparticles binding on the bacterial cell surfaces.

200 μg/ml conc. There was no delay in hatching observed for the lesser conc. but in case of higher conc. the coagulations observed along with reddish purple color changes noted (Fig. 10c). Further, the embryos treated with $CuSO_4{\cdot}5H_2O$ and CuNPs observed 100% of the mortality rate at the least conc of 2 μg/ml along with black color coagulations (Fig. 10d & e). However, we did not observe any kind of tail malformations and yolk sac edema against all the tested conc. of the nanoparticles.

4. Discussion

For the nanoparticle's formation, pH, concentration of leaves extract, concentration of substrate and time were noted in which 12 ml of the extract with 38 ml of $D{\cdot}H_2O$ was found to be suitable for rapid synthesis of both AuNPs and CuNPs. pH is one of the foremost factors for the rapid and controlled synthesis of nanoparticles. Hence in the present study, pH 6–10 monitored for the synthesis of both AuNPs and CuNPs in which the color formation was observed in all the pH for AuNPs but the prominent absorption peak at 540 nm as well as band intensity was not achieved at pH 6, 7, 9 and 10. In case of pH 8, a prominent absorption peak as well as the band intensity was achieved consistently during the incubation of reaction solution in the dark condition. In our previous report, we had synthesized AuNPs using two different plant leaves extracts namely, *Cucurbita pepo* and *Malva crispa* and recorded the absorption peak at 540 nm with a suitable pH 7 and 8 (Krishnaraj et al., 2019). Similarly, for CuNPs synthesis, the color change from pale yellow to green as well as the characteristic absorption peak at 327 nm was achieved at pH 7 and 8. Such color changes and the characteristic absorption peak did not observe at pH 6, 9 and 10. To support the present findings, Ghosh et al. (2020) synthesized CuNPs from *Jatropha curcas* leaves extract and observed the characteristic absorption peak at 337 nm. The intensity of the pinkish violet color for AuNPs and green color for CuNPs were increased continuously during incubation was the sign of surface plasmon resonance (SPR) excitation trigger and the reduction of substrates into the reaction mixtures (Krishnaraj et al., 2010).

The results of the electron microscopic studies revealed the presence of poly disperse AuNPs and CuNPs without having any agglomeration and this was due to the presence of variety of phytochemicals in the reaction mixture (Caesar and Cech, 2016; Kil et al., 2017) such as flavanones, linear angular coumarins, prenylated chalcones, vitamins and minerals (Tattao et al., 2020), and also having the unique bioactive component of chalcones which is a flavanone group having aromatic ketone (Chavan et al., 2016) might reacted as capping and stabilizing agents. For supporting the present study, recently Paul et al. (2015) synthesized AuNPs using *Pogestemon benghalensis* leaves extract and confirmed the spherical and triangular shape of nanoparticles with an average size of 10–50 nm. In addition, Chung et al. (2017) synthesized spherical shaped CuNPs with the average size of 23–57 nm using *Eclipta prostrata* leaves extract.

The results of EDS profile spectrum clearly demonstrated that some of the weak signals along with Au such as N, O, S, Si and C (Supplementary Fig. S2) were achieved from AuNPs reaction mix-

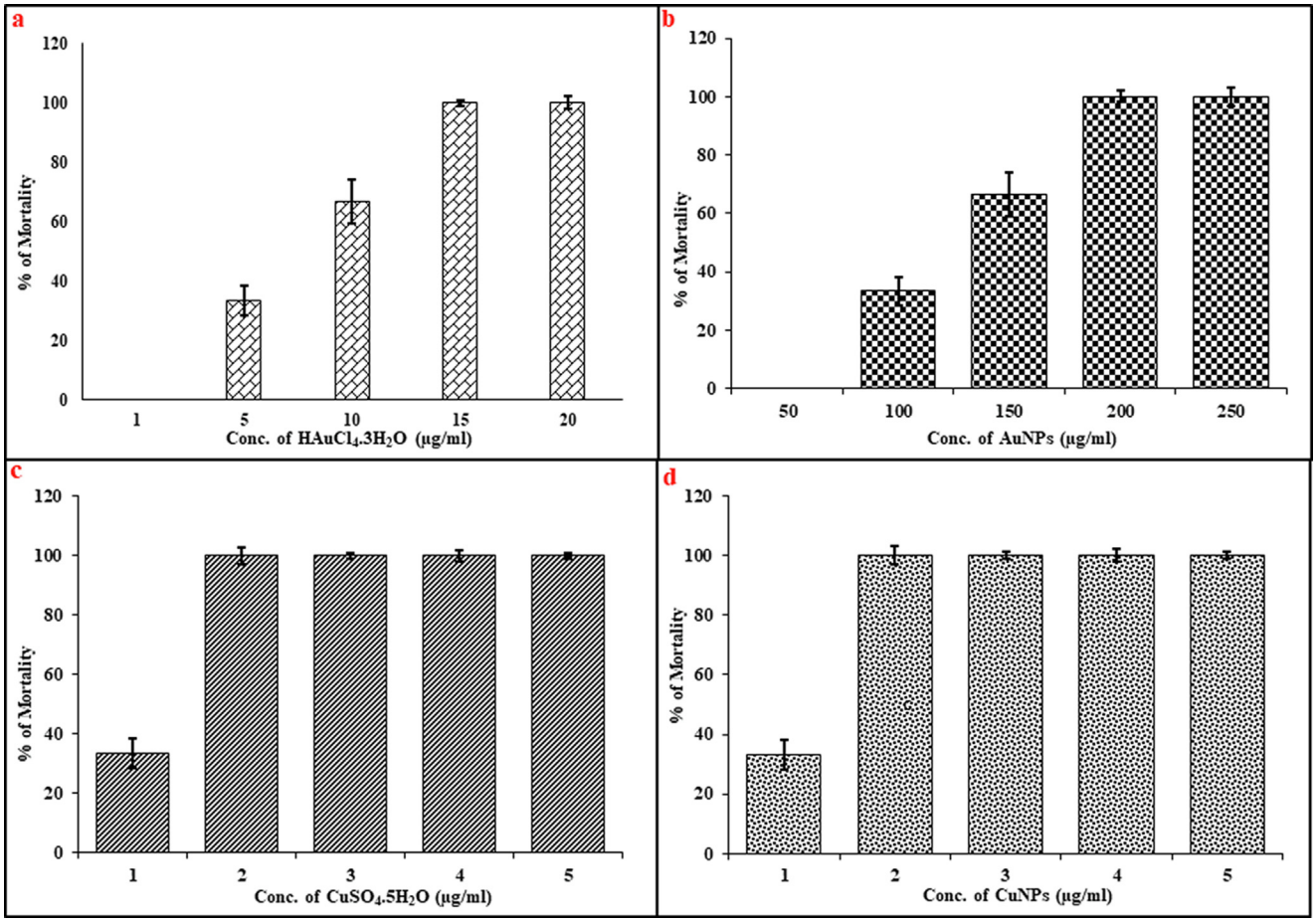

Fig. 9. Mortality rate of *A. keiskei* leaves extract mediated nanoparticles against zebrafish embryos (a) $HAuCl_4{\cdot}3H_2O$ exhibited 100% mortality at 15 µg/ml conc (b) AuNPs exhibited 100% mortality at 200 µg/ml conc (c) $CuSO_4{\cdot}5H_2O$ exhibited 100% mortality at 2 µg/ml conc (d) CuNPs exhibited 100% mortality at 2 µg/ml conc.

ture. Similarly, in case of CuNPs, some of the weak signals along with Cu such as C, Ca, N, O, Si, P, S and K (Supplementary Fig. S3) were observed and these might be due to the presence of phytochemicals adhered on the surface of nanoparticles (Caesar and Cech, 2016; Tattao et al., 2020; Chavan et al., 2016). Some of the previous reports also confirmed that the nanoparticles from the plant extract had a thin layer of surface capping organic molecules, which played a major role in nanoparticles stability in the solution for at least 1 month (Shankar et al., 2004; Song and Kim, 2009). Our results were in good agreement with the previous reports; AuNPs and CuNPs were found to be stable for more than 6 months (Supplementary Fig. S7).

The HR-XRD results clearly revealed the presence of few of the additional signals along with a characteristic plane for AuNPs and CuNPs. The additional signals were might be due to the presence of phytochemicals adhered on the surface of the nanoparticles. Singh et al. (2018) had synthesized AuNPs from *Euphrasia officinalis* leaves extract and confirmed the crystalline nature of fcc Au with JCPDS file No. 04-0784. In addition, recently Ghosh et al. (2020) had synthesized CuNPs from *Jatropha curcas* leaves extract and characterized the crystalline phase of the nanoparticles through XRD and confirmed the fcc matched with the JCPDs file No. 89-5899.

A characteristic band in the FTIR analysis of the plant leaves extract was observed between 3300 and 3600 cm^{-1} which confirmed the alcoholic –OH groups. In addition, the sharp C–N stretching vibration of aliphatic amines were observed at 1050 cm^{-1}. A medium peak formed at 1090 to 1150 cm^{-1} confirmed the presence of phenolic substances in the plant extract. The region between 1300 and 1450 cm^{-1} represented the confirmation of C–N stretching for aromatic amines and germinal methyl groups. Further the presence of C=C and C–H stretching functional groups of benzene was identified between 1590 and 1650 cm^{-1} and 2800 to 2900 cm^{-1}, respectively. In case of AuNPs, the significant bands were observed at 750 cm^{-1} to 600 cm^{-1}, 1633 cm^{-1} and 3378 cm^{-1}. The band at 3378 cm^{-1} confirmed the presence –OH bond on the AuNPs. The bands between 750 and 600 cm^{-1} were due to the presence of alkyl halides and band at 1633 cm^{-1} - signify the existence of amide group. In addition, some of the strong and broad signals observed between the region of 1600–1700 cm^{-1} confirms the presence of C=O group. Similarly, for CuNPs, the specific peaks were observed at 3365, 1718, 1628, 1145, 1098, 775 and 617 cm^{-1}. The major absorption peaks of CuNPs observed at 3600 cm^{-1} and 3000 cm^{-1} indicates the presence of alcohols associated with –OH and –NH stretching.

Recenlty, Amaliyah et al. (2020) have synthesized CuNPs from *Piper retrofractum vahl* extract as bio reducer and capping agent and performed the antibacterial activity against *Escherichia coli* and *Staphylococcus aureus* and reported the strong antibacterial activity against Gram-negative bacteria than the Gram-positive bacteria due to the difference in the membrane structure. Similarly, an effective antibacterial activity was observed against Gram-negative bacteria than the Gram-positive bacteria for AuNPs synthesized using *Lignosus rhinocerotis* and chitosan (Katas et al., 2019). Our results agree with the previous reports in which effective antibacterial activity of CuNPs and AuNPs was observed

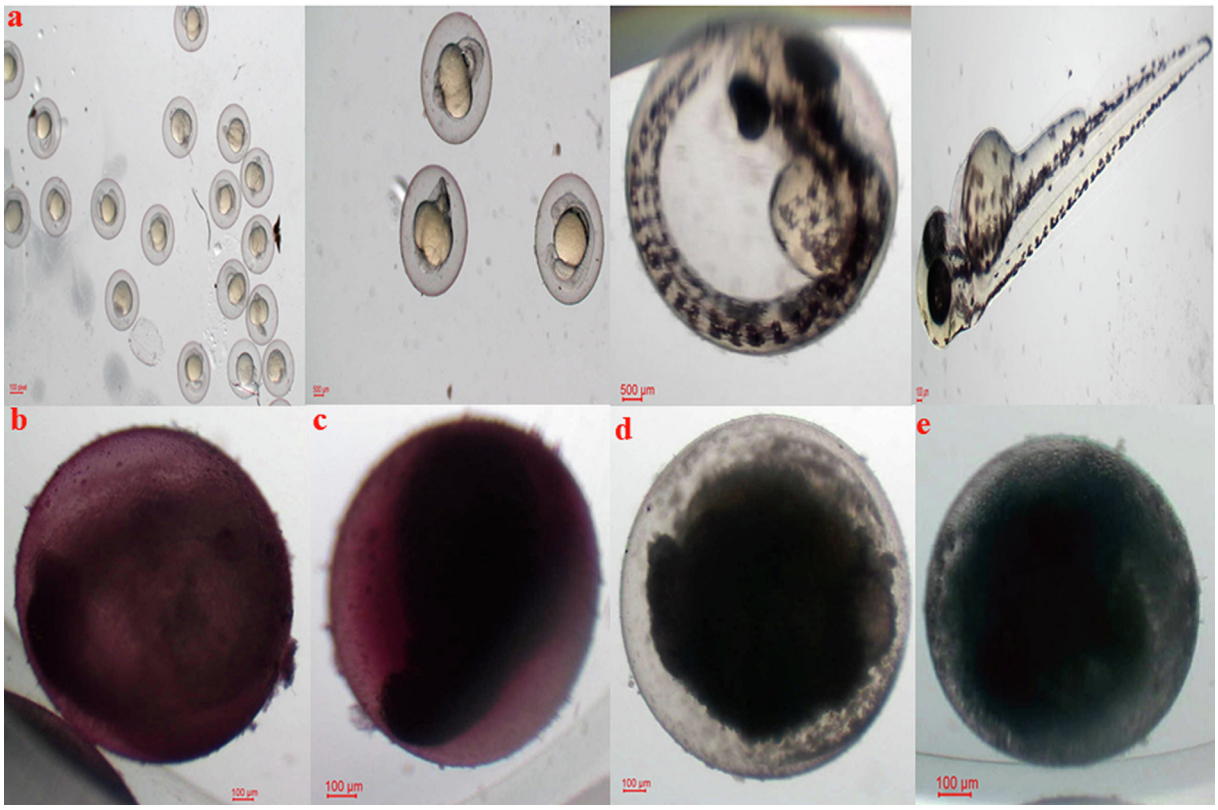

Fig. 10. Morphological anomalies caused by *A. keiskei* leaves extract mediated nanoparticles (a) Control embryos showed normal architecture at different developmental stages and coagulation caused by (b) $HAuCl_4{\cdot}3H_2O$ (c) AuNPs (d) $CuSO_4{\cdot}5H_2O$ (e) CuNPs.

against Gram-negative bacteria than the Gram-positive bacteria. This might be due to easy penetration of smaller size of nanoparticles into the thin cell wall of Gram-negative bacteria, which made them more susceptible to nanoparticles than the thick peptidoglycan layer of the Gram-positive bacteria (Katas et al., 2019; Muthuvel et al., 2014; Kaviya et al., 2011). In addition, presence of a rich variety of bioactive components found in the leaves extract might have contributed to the effective inhibitory activities. Moreover, Wu et al. (2020) had synthesized CuNPs from *Cissus vitiginea* Linn. leaves extract and reported the potent antioxidant properties and antibacterial activity against UTI infection caused by *E. coli, Enterococcus* sp., *Proetus* sp., and *Klebsiella sp*. For supporting the present proposal of the antibacterial mechanisms, few of the previous reports also concluded that CuNPs and ions of copper primarily adhered on the surface of bacterial cell and leads to pits formation on the bacterial membrane, leakage in cellular components as well as oxidative stress resulting in cell death (Deryabin et al., 2013; Saleem et al., 2017). In addition, CuNPs interact with the cell membrane leads to electrochemical transmembrane potential and resulted in membrane integrity. In another study, the proteins and enzymes were destroyed in the bacterial cell due to CuNPs interaction with -SH (sulfhydryl) group (Das et al., 2010; Schrand et al., 2010; Din et al., 2017).

In our previous report, we have reported the biological synthesis of silver and gold nanoparticles using *Spinacia oleracea* Linn. leaves extract and studied the embryotoxicity against zebrafish and confirmed that the 3 µg/ml concentration of silver nanoparticles and 300 mg/ml concentration of AuNPs were toxic to embryos resulted in 100% mortality (Ramachandran et al., 2017). But, in the present study, 100% mortality was observed for AuNPs at 200 µg/ml concentration and this might be due to the possibility of the nature and type of phytochemicals adhered on the surface of the nanoparticles.

5. Conclusions

Both AuNPs and CuNPs were successfully synthesized from *Angelica keiskei* (Miq.) Koidz. leaves extract. AuNPs were found to be triangular and spherical in shape with polydisperse in nature and the size was ranged from 10 to 40 nm whereas CuNPs were found to be spherical in shape with polydisperse in nature and the size was ranged from 10 to 60 nm. The antibacterial mechanisms of the synthesized AuNPs and CuNPs were investigated against few of the bacterial pathogens and their mode of interaction was performed using Bio-TEM. Based on the results obtained from various antibacterial mechanistic studies confirmed that the plant extracts mediated synthesis of AuNPs and CuNPs were found to be more effective against Gram-negative bacteria than the Gram-positive bacteria. Furthermore, *in vitro* embryotoxicity studies of the synthesized nanoparticles were performed against zebrafish embryos and the results concluded that 200 µg/ml concentration of AuNPs showed the embryotoxicity and 2 µg/ml of CuNPs resulted in embryotoxicity. Furthermore, the morphological anomalies of the zebrafish embryos confirmed the high toxic nature of the synthesized CuNPs than the AuNPs. Overall, AuNPs had the meager toxic effect than that of CuNPs even though both the nanoparticles were biosynthesized from the same plant. In addition, biologically synthesized AuNPs having the wide therapeutic uses and can be used at controlled concentration for various applications in biology.

Declaration of Competing Interest

The authors declare that they have no known competing financial interests or personal relationships that could have appeared to influence the work reported in this paper.

Acknowledgements

This project was supported by the Basic Science Research Program through National Research Foundation of Korea, NRF-2021R1A2C1094316. This project was also supported by research funds of Jeonbuk National University in 2019.

Appendix A. Supplementary material

Supplementary data to this article can be found online at https://doi.org/10.1016/j.sjbs.2021.12.039.

References

Abdullah, M.A.E., Ahamad, T., Al-hajji, A.B., Ahmed, J., Chaudhary, A.A., Alshehri, S. M., 2018. Cellulose gum and copper nanoparticles-based hydrogel as antimicrobial agents against urinary tract infection (UTI) pathogens. Int. J. Biol. Macromol. 109, 803–809. https://doi.org/10.1016/j.ijbiomac.2017.11.057.

Aerle, R.V., Lange, A., Moorhouse, A., Paszkiewicz, K., Ball, K., Johnston, B.D., Bastos, E.D., Booth, T., Tyler, C.R., Santos, E.M., 2013. Molecular mechanisms of toxicity of silver nanoparticles in zebrafish embryos. Environ. Sci. Technol. 47, 8005–8014. https://doi.org/10.1021/es401758d.

Amaliyah, S., Pangesti, D.P., Masruri, M., Sabarudin, A., Sumitro, S.B., 2020. Green synthesis and characterization of copper nanoparticles using *Piper retrofractum Vahl* extract as bioreductor and capping agent. Heliyon. 6,. https://doi.org/10.1016/j.heliyon.2020.e04636 e04636.

Anbu, P., Gopinath, S.C.B., Jayanthi, S., 2020. Synthesis of gold nanoparticles using *Platycodon grandiflorum* extract and its antipathogenic activity under optimal conditions. Nanomater. Nanotechnol. 10, 1–9. https://doi.org/10.1177/1847980420961697.

Baba, K., Taniguchi, M., Nakata, K., 1998. Studies on *Angelica keiskei* "Ashitaba". Foods Food Ingred J. Jpn. 178, 52–60.

Bao, G., 2014. *Angelica keiskei*-containing nutritional and health protecting flour and its preparation method (Qingyang county nanyang rice industry Co., Ltd, Peop. Rep. China). Application: CN.

Botteon, C.E.A., Silva, L.B., Ccana-Ccapatinta, G.V., Silva, T.S., Ambrosio, S.R., Veneziani, R.C.S., Bastos, J.K., Marcato, P.D., 2021. Biosynthesis and characterization of gold nanoparticles using *Brazilian red propolis* and evaluation of its antimicrobial and anticancer activities. Sci. Rep. 11, 1974–1989. https://doi.org/10.1038/s41598-021-81281-w.

Bukhari, S.I., Hamed, M.M., Al-Agamy, M.H., Gazwi, H.S.S., Radwan, H.H., Youssif, A. M., 2021. Biosynthesis of copper oxide nanoparticles using *Streptomyces* MHM38 and its biological applications. J. Nanomater. 1–16. https://doi.org/10.1155/2021/6693302.

Caesar, L.K., Cech, N.B., 2016. A review of the medicinal uses and pharmacology of Ashitaba. Planta Med. 82, 1236–1245. https://doi.org/10.1055/s-0042-110496.

Chavan, B.B., Gadekar, A.S., Mehta, P.P., Vawhal, P.K., Kolsure, A.K., Chabukswar, A.R., 2016. Synthesis and medicinal significance of Chalcones- A review. Asian. J. Biomed. Pharm. Sci. 6, 01–07.

Cassar, S., Beekhuijzen, M., Beyer, B., Chapin, R., Dorau, M., Hoberman, A., Krupp, E., Leconte, I., Stedman, D., Stethem, C., Oetelaar, D., Tornesi, B., 2019. A multi-institutional study benchmarking the zebrafish developmental assay for prediction of embryotoxic plasma concentrations from rat embryo–fetal development studies. Reprod. Toxicol. 86, 33–44. https://doi.org/10.1016/j.reprotox.2019.02.004.

Chung, I.M., Rahuman, A.A., Marimuthu, S., Vishnu Kirthi, A., Anbarasan, K., Padmini, P., Rajakumar, G., 2017. Green synthesis of copper nanoparticles using *Eclipta prostrata* leaves extract and their antioxidant and cytotoxic activities. Exp. The Med. 14, 18–24. https://doi.org/10.3892/etm.2017.4466.

Cittrarasu, V., Kaliannan, D., Dharman, K., Maluventhen, V., Easwaran, M., Liu, W.C., Balasubramanian, B., Arumugam, M., 2021. Green synthesis of selenium nanoparticles mediated from *Ceropegia bulbosa Roxb* extract and its cytotoxicity, antimicrobial, mosquitocidal and photocatalytic activities. Sci. Rep. 11, 1032–1046. https://doi.org/10.1038/s41598-020-80327-9.

Das, R., Gang, S., Nath, S.S., Bhattacharjee, R., 2010. Linoleic acid capped copper nanoparticles for antibacterial activity. J. Bio-nanosci. 4, 82–86. https://doi.org/10.1166/jbns.2010.1035.

Deryabin, D.G., Aleshina, E.S., Vasilchenko, A.S., Deryabina, T.D., Efremova, L.V., Karimov, I.F., Korolevskaya, L.B., 2013. Investigation of copper nanoparticles antibacterial mechanisms tested by luminescent *Escherichia coli* Strains. Nanotech Russia. 8, 402–408. https://doi.org/10.1134/S1995078013030063.

Din, M.I., Arshad, F., Hussain, Z., Mukhta, M., 2017. Green adeptness in the synthesis and stabilization of copper nanoparticles: catalytic, antibacterial, cytotoxicity, and antioxidant activities. Nanoscale Res Lett. 12, 638. https://doi.org/10.1186/s11671-017-2399-8.

Ghosh, M.K., Sahu, S., Gupta, I., Ghorai, T.K., 2020. Green synthesis of copper nanoparticles from an extract of *Jatropha curcas* leaves: characterization, optical properties, CT-DNA binding and photocatalytic activity. RSC Adv. 22027–22035. https://doi.org/10.1039/D0RA03186K.

Gulson, B., McCall, M., Korsch, M., Gomez, L., Casey, P., Oytam, Y., Taylor, A., McCulloch, M., Trotter, J., Kinsley, L., Greenoak, G., 2010. Small amounts of zinc from zinc oxide particles in sunscreens applied outdoors are absorbed through human skin. Toxicol Sci. 118, 140–149. https://doi.org/10.1093/toxsci/kfq243.

Henriquez, L.C., Aguilar, K.A., Alvarez, J.U., Fernandez, L.V., Vasquez, G.M.O., Baudrit, J.R.V., 2020. Green synthesis of gold and silver nanoparticles from plant extracts and their possible applications as antimicrobial agents in the agricultural area. Nanomaterials. 10, 1763. https://doi.org/10.3390/nano10091763.

Imai, K., Imai, M., 2008. Encyclopedia of wild herbs and vegetables. Green Home, Seoul.

Katas, H., Lim, C.S., Azlan, A.Y.H.N., Buang, F., Busra, M.F.M., 2019. Antibacterial activity of biosynthesized gold nanoparticles using biomolecules from *Lignosus rhinocerotis* and chitosan. Saudi. Pharm. J. 27, 283–292. https://doi.org/10.1016/j.jsps.2018.11.010.

Kimura, Y., Baba, K., 2003. Antitumor and antimetastatic activities of *Angelica keiskei* roots, Part 1: isolation of an active substance, xanthoangelol. Int. J. Cancer. 106, 429–437. https://doi.org/10.1002/ijc.11256.

Kil, Y.S., Pham, S.T., Seo, E.K., Jafari, M., 2017. *Angelica keiskei*, an emerging medicinal herb with various bioactive constituents and biological activities. Arch. Pharm. Res. 40, 655–675. https://doi.org/10.1007/s12272-017-0892-3.

Krishnaraj, C., Jagan, E.G., Rajasekar, S., Selvakumar, P., Kalaichelvan, P.T., Mohan, N., 2010. Synthesis of silver nanoparticles using *Acalypha indica* leaf extracts and its antibacterial activity against water borne pathogen. Colloids Surf B Biointerfaces. 76, 50–56. https://doi.org/10.1016/j.colsurfb.2009.10.008.

Krishnaraj, C., Jagan, E.G., Ramachandran, R., Abirami, S.M., Mohan, N., Kalaichelvan, P.T., 2012. Effect of biologically synthesized silver nanoparticles on *Bacopa monnieri* (Linn.) Wettst. plant growth metabolism. Process Biochem. 47, 651–658. https://doi.org/10.1016/j.procbio.2012.01.006.

Krishnaraj, C., Harper, S.L., Yun, S.I., 2016. In Vivo toxicological assessment of biologically synthesized silver nanoparticles in adult Zebrafish *(Danio rerio*). J . Hazard Mater. 301, 480–491. https://doi.org/10.1016/j.jhazmat.2015.09.022.

Krishnaraj, C., Seonhwa, S., Yun, S.I., 2019. Effect of size and shape controlled biogenic synthesis of gold nanoparticles and their mode of interactions against food borne bacterial pathogens. Arabian J. Chem. 12, 1994–2006. https://doi.org/10.1016/j.arabjc.2014.11.041.

Ku, C.S., Kim, M.J., Jung, Y.J., Jang, D.I., 2014. Cosmetic compositions containing *Angelica keiskei* extracts (COTDE Co., Ltd., S. Korea). Application: KR.

Lammer, E., Carr, G.J., Wendler, K., Belanger, S.E., Braunbeck, T., 2009. Is the fish embryo toxicity test (FET) with the zebrafish *(Danio rerio*) a potential alternative for the fish acute toxicity test? Comp. Biochem. Physiol. C Toxicol. Pharmacol. 149, 196–209. https://doi.org/10.1016/j.cbpc.2008.11.006.

Liu, X., Wang, Z., Sun, J., Wan, Y., Rong, Y., 2014. Coix seed-*Angelica keiskei* nutritional health-care biscuits and production method thereof (Shanghai Jiao Tong University, Peop. Rep. China). Application: CN.

Kaviya, S., Santhanalakshmi, J., Viswanathan, B., Muthumary, J., Srinivasan, K., 2011. Biosynthesis of silver nanoparticles using *citrus sinensis* peel extract and its antibacterial activity. Spectrochim. Acta. A. Mol. Biomol. Spectrosc. 79, 594–598. https://doi.org/10.1016/j.saa.2011.03.040.

Milanezi, F.G., Meireles, L.M., Christo Scherer, M.M., Oliveira, J.P., Silva, A.R., Araujo, M.L., Endringer, D.C., Fronza, M., Guimaraes, M.C.C., Scherer, R., 2019. Antioxidant, antimicrobial and cytotoxic activities of gold nanoparticles capped with quercetin. Saudi Pharm J. 27, 968–974. https://doi.org/10.1016/j.jsps.2019.07.005.

Muthuvel, A., Adavallan, K., Balamurugan, K., Krishnakumar, N., 2014. Biosynthesis of gold nanoparticles using *Solanum nigrum* leaf extract and screening their free radical scavenging and antibacterial properties. Biomed. Prev. Nutr. 4, 325–332. https://doi.org/10.1016/j.bionut.2014.03.004.

Narayanan, K.B., Sakthivel, N., 2010. Phytosynthesis of gold nanoparticles using leaf extract of *Coleus amboinicus* Lour. Mater Char. 61, 1232–1238. https://doi.org/10.1016/j.matchar.2010.08.003.

Navarro, E., Baun, A., Behra, R., Hartmann, N.B., Filser, J., Miao, A.J., Quigg, A., Santschi, P.H., Sigg, L., 2018. Environmental behavior and ecotoxicity of engineered nanoparticles to algae, plants, and fungi. Ecotoxicology 17, 372–386. https://doi.org/10.1007/s10646-008-0214-0.

Ogunyemi, S.O., Abdallah, Y., Zhang, M., Fouad, H., Hong, X., Ibrahim, E., Masum, M. M.I., Hossain, A., Mo, J., Li, B., 2019. Green synthesis of zinc oxide nanoparticles using different plant extracts and their antibacterial activity against *Xanthomonas oryzae* pv. Oryzae. Artif cells Nanomed. Biotechnol. 47, 341–352. https://doi.org/10.1080/21691401.2018.1557671.

Park, J.C., 2013. The medicinal herbs, teas, and alcoholic beverages in Donguibogam, proven by patents, Pureun-Hyeongbok Publisher, Goyang.

Paul, B., Bhuyan, B., Purkayastha, D.D., Dey, M., Dhar, S.S., 2015. Green synthesis of gold nanoparticles using *Pogestemon benghalensis* (B) O. Ktz. leaf extract and studies of their photocatalytic activity in degradation of methylene blue. Mater. Lett. 148, 37–40. https://doi.org/10.1016/j.matlet.2015.02.054.

Rajeshkumar, S., Menon, S., Venkat Kumar, S., Tambuwala, M.M., Bakshi, H.A., Mehta, M., Satija, G., Gupta, G., Chellappan, D.K., Thangavelu, L., Dua, K., 2019. Antibacterial and antioxidant potential of biosynthesized copper nanoparticles mediated through *Cissus arnotiana* plant extract. J. Photochem. Photobiol. B Biol. 197,. https://doi.org/10.1016/j.jphotobiol.2019.111531 111531.

Ramachandran, R., Krishnaraj, C., Sivakumar, A.S., Prasannakumar, P., Abhay Kumar, V.K., Shim, K.S., Song, C.G., Yun, S.I., 2017. Anticancer activity of biologically synthesized silver and gold nanoparticles on mouse myoblast cancer cells and their toxicity against embryonic zebrafish. Mater. Sci. Eng. C. 73, 674–683. https://doi.org/10.1016/j.msec.2016.12.110.

Rashmi, B.N., Harlapur, S.F., Avinash, B., Ravikumar, C.R., Nagaswarupa, H.P., Anil Kumar, M.R., Gurushantha, K., Santosh, M.S., 2020. Facile green synthesis of silver oxide nanoparticles and their electrochemical, photocatalytic and biological studies. Inorg. Chem. Commun. 111,. https://doi.org/10.1016/j.inoche.2019.107580 107580.

Saleem, S., Ahmed, B., Khan, M.S., Shaeri, M.A., Musarrat, J., 2017. Inhibition of growth and biofilm formation of clinical bacterial isolates by NiO nanoparticles synthesized from *Eucalyptus globulus* plants. Microb. Pathog. 111, 375–387. https://doi.org/10.1016/j.micpath.2017.09.019.

Schaffler, M., Sousa, F., Wenk, A., Sitia, L., Hir, S., Schleh, C., Haberl, N., Violatto, M., Canovi, M., Andreozzi, P., Salmona, M., Bigini, P., Kreyling, W.G., Krol, S., 2014. Blood protein coating of gold nanoparticles as potential tool for organ targeting. Biomaterials 35, 3455–3466. https://doi.org/10.1016/j.biomaterials.2013.12.100.

Schrand, A.M., Rahman, M.F., Hussain, S.M., Schlager, J.J., Smith, D.A., Syed, A.F., 2010. Metal-based nanoparticles and their toxicity assessment. Nanomed. Nanobiotechnol. 2, 544–568. https://doi.org/10.1002/wnan.103.

Shankar, S.S., Rai, A., Ahmad, A., Sastry, M., 2004. Rapid synthesis of Au, Ag and bimetallic Au core-Ag shell nanoparticles using Neem *(Azadirachta indic*a) leaf broth. J. Colloid Interface Sci. 275, 496–502. https://doi.org/10.1016/j.jcis.2004.03.003.

Singh, H., Dua, J., Singh, P., Yi, T.H., 2018. Ecofriendly synthesis of silver and gold nanoparticles by *Euphrasia officinalis* leaf extract and its biomedical applications. Artif. cells Nanomed. Biotechnol. 46, 1163–1170. https://doi.org/10.1080/21691401.2017.1362417.

Song, J.Y., Kim, B.S., 2009. Rapid biological synthesis of silver nanoparticles using plant leaf extract. Bioprocess Biosyst. Eng. 32, 79. https://doi.org/10.1007/s00449-008-0224-6.

Su, L., 2014. A method for preparing *Angelica keiskei* wine (Nanjing Zelang Agriculture Development Co., Ltd., Peop. Rep. China). Application: CN.

Tattao, J.A.M., Velasco, R.V., Doctolero, J.S., 2020. Potential of ashitaba *(Angelica keiskei Koidzumi*) leaves as a feed additive on the diet of Nile tilapia fry *(Oreochromis niloticus* L.). Int. J. Fisheries Aquat. Stud. 8, 16–19.

Usman, M.S., Zowalaty, M.E.E., Shameli, K., Zainuddin, N., Salama, M., Ibrahim, N.A., 2013. Synthesis, characterization, and antimicrobial properties of copper nanoparticles. Int. J. Nanomed. 8, 4467–4479. https://doi.org/10.2147/IJN.S50837.

Veena, S., Devasena, T., Sathak, S.S.M., Yasasve, M., Vishal, L.A., 2019. Green synthesis of gold nanoparticles from *Vitex negundo* leaf extract: characterization and *in vitro* evaluation of antioxidant-antibacterial activity. J. Cluster Sci. 30, 1591–1597. https://doi.org/10.1007/s10876-019-01601-z.

Vincent, M., Hartemann, P., Deutsch, M.E., 2016. Antimicrobial applications of copper. Int. J. Hyg. Environ. Health. 219, 585–591. https://doi.org/10.1016/j.ijheh.2016.06.003.

Wu, S., Rajeshkumar, S., Madasamy, M., Mahendran, V., 2020. Green synthesis of copper nanoparticles using *Cissus vitiginea* and its antioxidant and antibacterial activity against urinary tract infection pathogens. Artif. Cells Nanomed. Biotechnol. 48, 1153–1158. https://doi.org/10.1080/21691401.2020.1817053.

Xia, G., Liu, T., Wang, Z., Hou, Y., Dong, L., Zhu, J., Qi, J., 2016. The effect of silver nanoparticles on zebrafish embryonic development and toxicology. Artif. Cells Nanomed. Biotechnol. 44, 1116–1121. https://doi.org/10.3109/21691401.2015.1011803.

Yasmin, A., Ramesh, K., Rajeshkumar, S., 2014. Optimization and stabilization of gold nanoparticles by using herbal plant extract with microwave heating. Nano Converg. 1, 12. https://doi.org/10.1186/s40580-014-0012-8.